Synthetic Polymer-Polymer Composites

Editors

DEBES BHATTACHARYYA and STOYKO FAKIROV
Center of Advanced Composite Materials, University of Auckland, New Zealand

ISBN (Book): 978-1-56990-510-4
ISBN (E-Book): 978-1-56990-525-8
HANSER PUBLISHERS, Munich

Chapter 8

Chapter 8

Manufacturing and Properties of Aramid Reinforced Composites

Z. Denchev, N. Dencheva

8.1. Introduction

The development of *aromatic polyamides* (*aramids*) had its beginning in the early 1960s in an industrial corporation (DuPont) and was a combination of fundamental science, engineering, and applications research from its very early stages. The broad range of properties of aramids and their structural variety are the main reason for their utility in diverse applications [1].

The key property of aramid fiber reinforced composites in comparison with other fiber containing polymers is the cost-effective performance at reduced weight. Glass fibers, for example, are much cheaper but display lower strength and modulus, increasing also the weight. Carbon fibers have the highest strength and modulus of the three fiber types, but show the lowest elongation and are more expensive than aramids. Aramid fibers possess a unique combination of high strength and modulus with low density and high elongation that results in improved impact resistance of the respective composites. Together with the different carbon fiber grades, aramid fibers are the dominant reinforcement in fiber reinforced polymers (FRP) for demanding applications in aerospace industry where excellent mechanical properties per unit weight are required [2]. Thus, in aircrafts, aramid fibers are used in FRP for storage bins, air ducts, in a variety of core (honeycomb) structures, as well as in secondary aircraft structures. Aramids high tensile strength lends itself well to the manufacture of sporting goods where weight can be reduced significantly while providing greater tear strength and puncture resistance than fiberglass composites. Sailing boat fuselages, hockey shafts, golf club shafts, fishing rods, and tennis rackets have incorporated aramid composites. In skis, aramid fibers dampen vibration for smoother,

more comfortable skiing [3]. Some aramid containing composite materials are useful as thermal- and heat-resisting barriers, others for elastomer reinforcement.

In most of the above composites, as polymer matrices, thermoset polymers have gained major industrial importance as matrix materials. The use of thermoplastic matrices for aramid FRPs is being increasingly studied recently. There are also a vast number of applications where aramid fibers are the sole constituent, *e.g.*, in protective apparel, armor systems, ropes, *etc.* During the last decade the aramid containing FRP composites have developed into economically and structurally viable construction materials for buildings and bridges [4].

The functional properties of the aramid-reinforced polymer composites depend primarily on the properties of the aramid reinforcing fibers, since the fraction of the fiber constituent in FRP is quite high, usually well above 30% by volume. The properties of the aramid fibers, in turn, depend on their chemical composition and manufacturing conditions: both of these determine the fibers physical structure and mechanical properties. The chapter will focus on these issues. Some specific problems related to the fiber-matrix interaction in aramid-containing FRP will also be addressed.

8.2. Aramid types and manufacturers

The superior properties of aramid materials were the reason why significant research effort has been devoted to their synthesis. In 1989 there were at least 100 different chemical compositions of aromatic and aromatic-aliphatic polyamides [5] and there are indications that the number has doubled until today. This fact led the U.S. Federal Trade Commission to adopt a definition for "aramid" designating fibers of the aromatic polyamide type in which at least 85% of the amide linkages are attached directly to two aromatic rings. The compounds corresponding to this definition that have reached commercial stage are only four (Scheme 8.1): poly(*m*-phenylene isophthalamide) (MPDI), poly(*p*-phenylene terephthalamide) (PPTA), copoly(*p*-phenylene-3,4-diphenyl ether terephthalamide) (ODA-PPTA), and poly[5-amino-2(*p*-aminophenyl) benzimidazole terephthalamide] (SVM). The process of commercialization of every compound has always been the result of a constant trade-off between properties, processability and price.

The basic development and the first commercial introduction of aramid materials were done by DuPont, which continues to be the largest producer. MPDI fiber products (staple, continuous filament, yarn, and floc) under the trademark Nomex® are produced by DuPont in the United States and Spain. The only other major MPDI producer is Teijin, with its fiber product Teijinconex® produced in Japan. The situation is very similar with the PPTA manufacturers. The first and largest manufacturer, DuPont, produces essentially all product forms except films. DuPont's PPTA fibers are known under the trademark Kevlar®. *p*-Aramid fiber is also produced in Ireland and Japan. The other producer of PPTA is Teijin Co., which produces two basic fibers: Twaron® based on PPTA, and Technora® based on the ODA-PPTA copolymer. A small amount of *p*-aramid fibers (Armos® and Rusar®) are produced in Russia, both being based on SVM copolymer [6].

It is interesting to note here that along with the aramids there exist other chemistries from which fiber materials with impressive properties can be developed. In the 1980s a poly(benzoxazole) yarn (PBO) was invented. Presently it is produced by Toyobo under

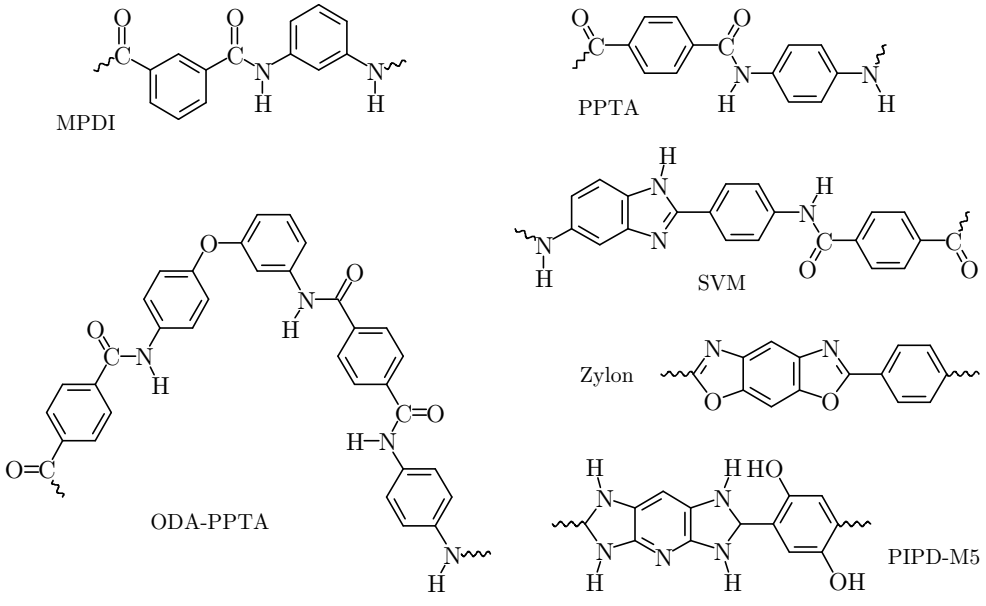

Scheme 8.1. Most important aramid structures of commercial importance: MPDI = poly(*m*-phenylene isophthalamide); PPTA = poly(*p*-phenylene terephthalamide); ODA-PPTA = copoly(*p*-phenylene/3,4′-diphenylether terephthalamide); SVM = poly[5-amino-2(*p*-aminophenyl)benzimidazole terephthalamide]. For Zylon and PIPD-M5 see the text

the trade name of Zylon®. Fibers based on the rigid-rod polymer poly[di-imidazo-pyridinylene (dihydroxy)phenylene] (PIPD or M5) are currently produced by Magellan Systems International, a subsidiary company of DuPont. Despite the fact that the chemical structures of Zylon and M5 (Scheme 8.1) cannot be considered aramidic, these fibers are even more rigid than those of *p*-aramids. This, however, is achieved at the expense of ease of processability and at a significantly higher cost. Picken *et al.* [7] gave the estimated production volumes of some high-performance fibers around the year 2001. The total amount of PPTA yarns produced was about 30 000 tons. Both Zylon and Rusar were estimated to have a volume of 400 t each. Since then, the PPTA increased to 40 000 tons while M5 is still being produced in a pilot scale [8]. Apparently, fiber materials of the Zylon and M5 type or even the PPTA-based copolymers will not replace *p*-aramids but most likely will be an important supplement to them.

8.3. Synthesis of aramids

The usual synthetic method for aliphatic polyamides by melt polycondensation is not suitable for preparing high molecular weight aramids because of their very high melting point and the reduced reactivity of the aromatic amine reagents. Polymerization of wholly aromatic polyamides is therefore carried out in solution using highly reactive diacid chlorides instead of the respective diacids. To obtain PPTA and MPDI homo- or copolymers,

the selected isomers of phthaloyl chloride and phenylenediamine are reacted typically at low temperature (from 0 °C to –40 °C) in order to avoid side reactions. There exist two ways of major industrial importance to perform the polymerization: the interfacial and the solution processes.

In the interfacial method, the two fast-reacting intermediates are dissolved in a pair of immiscible liquids, one of which is preferably water. The water phase contains the diamine and any added alkali. The second phase consists of the diacid halide in an organic liquid such as carbon tetrachloride, dichloromethane, xylene, hexane, *etc.* The two solutions are brought together with vigorous agitation and the reaction takes place at or near the interface of the two phases. Variables strongly affecting the interfacial polymerization include temperature, monomer ratio and concentration, impurities, additives, acid acceptor, and mode of addition. The impact of these and other factors on the molecular weight and the mechanical properties of the aramids are discussed in detail by Morgan [9]. The interfacial process has various advantages, *e.g.*, low reaction temperatures, little or no sensitivity to reactant nonequivalence, easy neutralization of the HCl and amine hydrochloride with water-soluble inorganic bases. The *interfacial polymerization*, however, produces aramids with very broad distribution of molecular weights not suitable for the production of fibers used in aramid-reinforced composites.

The preferred solvents in the *solution polymerization* process are *N*,*N*-dimethyl acetamide (DMAc), *N*-methylpyrrolidone (NMP), hexamethyl phosphoric triamide (HMPA) or some mixtures thereof [10]. The low crystalline MPDI (*m*-aramids) are relatively easy to produce at low temperatures in DMAc, NMP or their mixtures. Obtaining PPTA of high molecular weight, highly crystalline and with narrow molecular weight distribution (*i.e.*, optimized for fiber production) by the low temperature method has been quite challenging due to the lower solubility of the *p*-aramid in amide-type solvents. Initially, the highly toxic and carcinogenic HMPA or its mixtures with NMP were used, which was a substantial obstacle for the process scale-up. Later on, a lower-toxic alternative was found by combination of NMP or DMAc with $CaCl_2$ as solubilizing aid. The latter apparently increases the polarity of NMP and DMAc by complexing with their carbonyl groups [3]. The presence of suitable acid receptors and the use of highly effective mixing equipment further enhance the molecular weight increase [1].

The reaction mechanism of the aramid preparation is the well-known Schötten-Baumann process performed with fully aromatic and bifunctional monomers (Scheme 8.2).

As seen from Scheme 8.2, the first step is the attack of the amine nitrogen at the carbonyl carbon of the acid halide. An amide linkage is formed from the transition complex **I** by eliminating HX. This HX transforms the opposing amine group into a quaternary ammonium salt (**II**) in this way excluding it from the polymerization process. For polymerization to continue, an acid acceptor (pyridine) can be used to regenerate the amine end. The previously mentioned polymerization solvents, DMAc and NMP, are often sufficiently basic to function as acid acceptors as well.

An alternative route to aromatic polyamides is the polyurethane-type hydrogen transfer reaction between an aromatic diisocyanate and a diamine [11]. The low-temperature reaction between them produces an intermediate polymer that loses carbon dioxide in a subsequent heating to form the aramid. This reaction is not widely used because of the

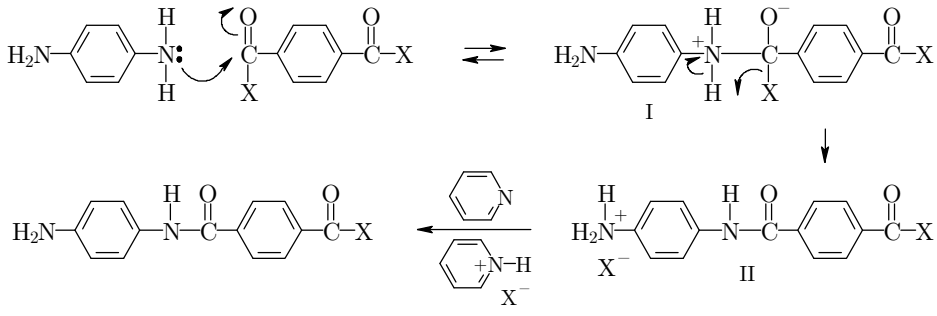

Scheme 8.2. Polymerization mechanisms of a *p*-diaminobenzene and terephthaloyl dichloride to get PPTA [3]

higher cost of diisocyanates and the difficulty in eliminating all the carbon dioxide from the final polymer.

Another polymerization scheme towards aramids not requiring transformation of the diacid into the more expensive and difficult to handle diacyl chlorides is possible with the so-called condensing agents. The latter, being derived from phosphorus and sulfur containing compounds, activate the aromatic acid *in situ* during polymerization [12]. The reaction has not been utilized commercially because the costs of recovering and regenerating the condensing agents by far outweigh the cost advantage of using unmodified diacids.

Two other noncommercialized high-temperature reaction paths deserve some attention. Vapor phase polymerization of aromatic diamines and diacylhalides [13] has the distinct advantage of not having to use solvent, making possible the elimination of the HCl by-product in the gas phase. However, the resulting aramid polymers are usually highly branched due to the high reaction temperature and useless for composite reinforcing. The plasticized melt polymerization route [14] is a unique procedure for preparing certain aromatic polyamides by a melt process using an internal plasticizer generated *in situ* during the polymerization. The melt polycondensation of isophthaloyl-*N*,*N*-bis-(valerolactam) with *m*-phenylene diamine yields MPDI aramid plasticized by the liberated valerolactam. The latter can be removed by water extraction after the shaping process, thereby recovering the infusible aromatic polyamide. More details about the reactive mechanisms of all polymerization processes toward aramids and about the synthesis routes of the respective starting reagents are given by Gabara *et al.* [3]. It can be verified that the production of most aramids is a highly integrated process that begins with the synthesis of the monomers and continues right to the production of their commercial forms.

8.4. Commercial forms of aramids and their physical properties

Yarns, films, fibrids, papers and pulp are the usual aramids commercial forms.

Aramid polymers have high melting points and melt with decomposition that makes impractical their processing to ***yarns*** (fibers) by melt spinning. Among the commercial aramids, only the flexible chain homo- and copolymers of MPDI type can be dissolved in NMP and DMAc [15] to form isotropic solutions transformed into yarns by a dry spinning

process [16]. Isotropic solutions can also be obtained with some *p*-aramids but only if they are copolymers, *e.g.*, in the case of the products of the SVM family and the Teijin's Technora (see Scheme 8.1). These copolymers remain soluble in their polymerization mixture so they can be dry-spun directly from that solution.

PPTA, however, is only soluble in strong acids and in highly polar solvents in the presence of inorganic salts forming anisotropic (*i.e.*, lyotropic or liquid crystalline) solutions. Thus, when PPTA polymer prepared by solvent polymerization in NMP/$CaCl_2$ solvent reaches $\overline{MW} \approx 40\,000$ g/mole, the polymer crystallizes and separates from the solution in the form of granules, which are then washed and dried, recovering the solvent. To produce yarns, the granules are dissolved in concentrated H_2SO_4 to form a 20% spinning solution. The heated spinning solution is extruded through spinnerets, stretched for orientation in an air gap and then coagulated in a nonsolvent. The mineral acid is washed out in aqueous coagulation/precipitation bath, and the orientation of the polymer chains is fixed as the filament yarn solidifies. The yarn is neutralized in further washing baths before being dried and wound onto bobbins. Standard types of yarn obtained comprise as many as 5 000 individual filaments, each one of them having an average diameter of 12 μm [17]. The spinning method called *dry-jet wet process* was patented by Blades in 1973 [18]. Aramid yarn is the most widely used commercial form for both *p*- and *m*-aramids. Their properties and application as reinforcements in FRP materials will be addressed separately in the next two subsections.

Aramid ***films*** have been in development since the late 1990s by several Japanese companies including Toray, Teijin, and Asahi. As with fibers, aramid solutions can be extruded through flat dies to form films. The conventional wet process can be employed to produce unidirectional and bi-oriented films from isotropic *m*-aramid solutions. It is more complicated to obtain isotropic *p*-aramid films. It requires extrusion of PPTA/H_2SO_4 solutions, which are exposed to subsequent steam treatment, bi-axial stretching, drying and specific annealing [19]. *p*-Aramid films have many applications in electrical industry.

Fibrids are film-like particles that are formed when aramid solutions are precipitated in a non-solvent under high shear [20,21]. The dimensions of as-formed fibrids are around 100 mm × 700 mm × 0.01 mm. Fibrids have a high surface area, around 200–300 m^2/g, and can function as a thixotrope or a reinforcing agent in composite, sealing, coating, and elastomer applications [22,23], and also in aramid papers.

Aramid ***papers*** are composed of a mixture of fibrids and short MPDA or PPTA fibers referred to as *floc*. MPDA aramid papers are used in aerospace industry to produce core structures used in a number of interior and exterior components of planes such as Boeing 747. Because of their superior compression, shear, and fatigue properties, structures based on *p*-aramid cores allow for even greater weight reduction than incumbent *m*-aramid cores. Recent commercial adoptions include flooring panels in weight critical programs such as the extended Airbus A-340 and the double deck Airbus A-380 [24].

For ***pulp*** manufacture, the PPTA yarn is chopped into short fibers, which are then suspended in water. The suspension passes through a refiner mill similar to the kind used in paper manufacture from wood pulp. In the mill aramid fibers are chopped even further, whereby the cutting action of the rotors gives rise to a random distribution of fiber length. At the same time, some crystalline domains partially detach themselves from the main

body of the fiber to form microfibrils [17]. Pulp retains the strength, stiffness, and thermal properties of the precursor fiber and, in addition, provides surface area of the order of 7–15 m^2/g. This high surface area serves as a processing aid in certain manufacturing steps and also as a retention aid for multicomponent composite formulations.

p-Aramids in the form of pulp are one of the few organic materials suited to the thermal demands of friction applications such as brake linings or pads, clutch facings, gaskets, *etc.* *p*-Aramid in pulp and short fiber forms is an effective reinforcing agent in both elastomer and thermoplastic resin matrices. Compared to traditional particulate reinforcing agents in elastomers such as carbon black and silica, aramid pulp provides superior reinforcement at much lower loadings [3]. Advantages of pulp-reinforced elastomers include high low-strain modulus, property anisotropy, greater cut and abrasion resistance, improved wear performance and, in tire stocks, lower rolling resistance. These attributes are achieved, however, only when the pulp is fully dispersed in the rubber matrix. Because high surface area pulp is rather difficult to break open and wet out by the conventional rubber compounding processes, concentrated pulp masterbatches have been formulated that allow compounders to more easily achieve adequate dispersion using standard mixing techniques. These masterbatches are available in natural and a variety of synthetic rubbers [25].

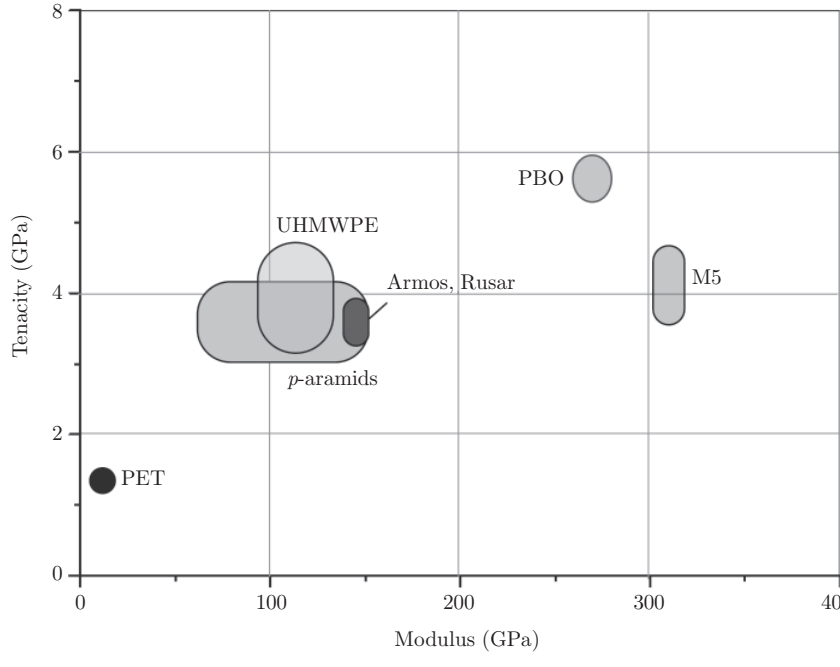

Figure 8.1. Overview of high performance fibers mechanical properties. PET = poly(ethylene terephthalate), UHMWPE = ultra-high molecular weight polyethylene, PBO = poly(benzoxazole), M5 = PIPD or poly[di-imidazo-pyridinylene-(dihydroxy phenylene)]. The *p*-aramids included in the area are Kevlar, Twaron, Technora and SVM (Armos, Rusar) fibers. The latter fiber type accounts for the high modulus/high tenacity area of aramids (Adapted from ref. [6]). For chemical structures see Scheme 8.1

8.5. Structure and properties of *p*-aramid fibers

In this subsection the physicochemical and mechanical properties of the most common *p*-aramid brands will be discussed. It is worth noting that mostly *p*-aramids are used for reinforcement of thermoset and thermoplastic polymer matrices where strength and stiffness are critical. However, in the case of elastomer-based composites where more important are the flame resistance, flexibility and the resistance to thermal, impulse and vibrational stresses, the *m*-aramid fiber reinforcement renders superior properties [3].

From Figure 8.1 [6] it can be seen that in terms of modulus and tenacity (*i.e.*, the tensile strength divided by the linear density) only the more expensive carbon fibers and some even more expensive, relatively new experimental heat-resistant fibers outperform the *p*-aramides. It is noteworthy that the oriented fibers of ultra-high molecular weight polyethylene (UHMWPE), *e.g.*, Dyneema®, a product of DSM, The Netherlands, display tenacities and moduli in the same range as most *p*-aramids, however without having their excellent thermal and flame-resistance, as well as insolubility in most organic solvents.

Table 8.1 [26] compares the mechanical properties, melting temperatures, and density of PPTA (Kevlar 981) and UHMWPE fibers with other types of inorganic fiber reinforcements. From the numerous grades of carbon fibers only the high-performance grades are shown, labeled "high strength (HS)" and "high modulus (HM)". Among the fibers (not counting the whiskers), HS carbon fibers exhibit the highest strength, while HM carbon fibers exhibit the highest modulus of elasticity. Moreover, the density of carbon fibers is quite low, making the specific modulus (modulus/density ratio) of HM carbon fibers quite high. The Kevlar and UHMWPE have exceptionally low densities compared to the other materials in Table 8.1, but their melting temperatures (especially of the latter) are relatively low. On the other hand, almost all ceramic fibers (except for the glass fibers) suffer from high prices or are not readily available in a continuous fiber form (*e.g.*, the whiskers).

Table 8.1. Properties of various fibers and whiskers used as reinforcements, based on information from [26]

Material	Density (g/cm^3)	Tensile strength (GPa)	Young's modulus (GPa)	Ductility (%)	Melting temp. (°C)
E-glass	2.55	3.4	72.4	4.7	<1725
S-glass	2.50	4.5	86.9	5.2	<1725
Carbon HS	1.50	5.7	280	2.0	3700
Carbon HM	1.50	1.9	530	0.4	3700
B_4C whiskers	2.52	14.0	480	2.9	2450
SiC whiskers	3.18	21.0	480	4.4	2700
Graphite whiskers	1.66	21.0	703	3.0	3700
Polyethylene	0.97	2.6	120	2.2	147
Kevlar 981	1.44	4.5	120	3.8	500

The main advantage of the mechanical properties of Kevlar PPTA over its main competitors the glass and carbon fibers is the superior specific strength, related to its low density.

There exist significant differences in the mechanical behavior among the most important PPTA fiber brands [21]. Clearly, only the *p*-aramids and their copolymers (*i.e.*, Kevlar, Twaron, Technora and SVM) possess the combination of high modulus (60–145 GPa) and high strength (2.7–4.5 GPa) necessary for advanced composite reinforcement. As to the flame resistance, apparently the copolymers Technora and SVM, and also the *m*-aramid (Nomex) are the best performing. With their limiting oxygen index (LOI) of above 30, they belong to the self-extinguishing materials. The modulus and strength of Nomex fibers, however, are significantly lower as compared to PPTA homo- and copolymers at 17.0 and 0.6 GPa, respectively [21].

These outstanding functional properties of the *p*-aramid fibers, in particular the excellent tensile properties, are directly related to their specific structure in various length scales. During the fiber manufacture by solution spinning and drawing through an air gap, the liquid crystalline domains orient and align in flow direction so the fiber produced is highly oriented, containing several levels of micro- and macroscopic structures.

On the level of the single macromolecule, the main chain of *p*-aramids is primarily built by aromatic rings and amide linkages. Due to steric hindrances, there is no rotation around the N-C bond of the amide groups, which in other polyamides is possible and results in *cis*-conformation of the amide linkage. Hence, in PPTA this linkage only stays in *trans*-conformation, *i.e.*, under normal conditions the macromolecules are extended and do not form kinks. Furthermore, since the C-N bond of the amide group of PPTA has partially double character [1], it conjugates with the aromatic ring double bonds, making the bond dissociation energies of the C-C and C-N bonds in the PPTA main chain significantly higher than those in aliphatic polyamides. These effects lead to the yellow color of the *p*-aramids, their increased chain rigidity and excellent thermal stability. At 300 °C, all Kevlar fibers retain about 50% of its strength at room temperature, while the modulus remains at 70% of this level [27].

Aramids do not melt in the conventional sense because decomposition occurs simultaneously. Thus, for Kevlar 49 in nitrogen atmosphere, the melting endotherm was observed in the DSC curves at ~580 °C followed by thermal decomposition, while in air, exothermic decomposition started at 489 °C, *i.e.*, far before melting [28]. As all polyamides, PPTA displays very good chemical resistance to the attack of most common organic solvents and aqueous salt solutions. Strong acids and bases, however, do attack aramid molecule at elevated temperatures, causing hydrolysis of the amide linkages and loss of strength. The aromatic nature of *p*-aramids is responsible for a substantial absorption of the UV light. This may lead to change of color due to photo oxidative reactions and drop in all fiber properties [1].

The formation of hydrogen bridges between the extended adjacent polymer chains in *p*-aramids ensures good cohesion between them and a high degree of orientation. Figure 8.2 shows an array of PPTA macromolecules, the dotted lines indicating the interaction of the hydrogen bridges that hold the polymer chains together forming a two-dimensional layered structure.

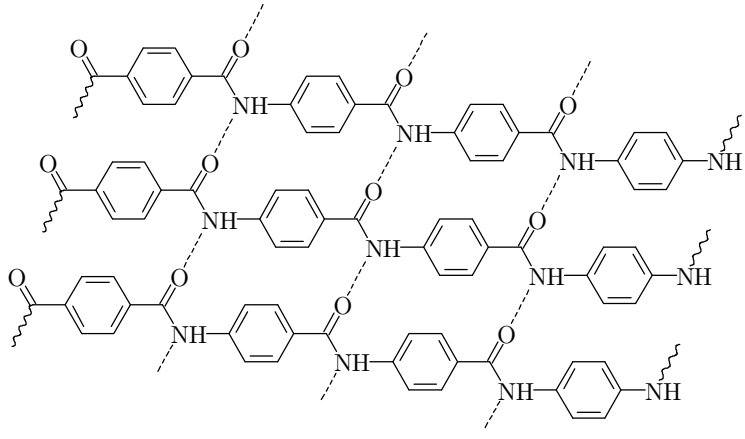

Figure 8.2. Hydrogen bond formation between adjacent PPTA macromolecules

p-Aramids are almost fully crystalline [29,30]. Unit cell parameters of various *p*-aramids are very similar and were determined in the early 1980s by various scientists [28,31], namely $a = 7.87$ Å, $b = 5.18$ Å, and $c = 12.9$ Å. The pseudo-orthorhombic (monoclinic) polymer crystal probably belongs to the $P2_1/m$ space group [28]. However, some weak reflections that do not obey the space group extinction rules were also found [31] resulting from stacking errors or conformational defects. The stacking occurs during the fiber manufacturing process, whereby the aramid solution is subjected to shear elongational flow, which (especially near the spinneret edges) aligns the domains along the flow direction joining them to form a fibrillar structure with a skin and core. Attenuation during spinning retains the highly directional molecular structure and gives rise to a highly orientated fiber structure with a large elastic modulus, high tenacity and thermal stability [30,32].

Dobb *et al.* [33], on conducting dark-field image techniques on PPTA fibers, found dark banding suggesting changes in crystallite orientation and compatibility with a regular pleated sheet structure. The dark field images showed evidence that the sheets are composed of alternating ingredients at equal, but opposite, angles to the section plane. Kevlar 49, in particular, had a radial system of pleated sheets. The presence of a pleated sheet structure can influence negatively the mechanical properties, particularly the elastic modulus. Dobb *et al.* mentioned also the absence of pleated sheet organization in those fibers of the Kevlar family with highest modulus (*e.g.*, Kevlar 149, Table 8.1). It was predicted that the presence of a radial sheet structure in some fibers would considerably influence the mode of mechanical failure and could be a contributory factor to the low compressive strength [33].

As mentioned above, the manufacturing process leaves aramid fibers with a skin/core structure, reflected in the model of Morgan *et al.* [32]. Apparently, the coagulation creates a differential in density, voidage and fibrillar orientation along the fiber cross section. The fiber surface cools more rapidly, and this, combined with the effects of solvent evaporation, leaves a skin layer with an average thickness between 0.1–0.6 μm, having low

crystallinity but with fibrils well oriented in axial direction. At the same time, the fibrils in the core are imperfectly packed and ordered. Based on their SEM study, Panar *et al.* suggested that although voids are probably present in the skin, the majority of them are found in the core [30].

Hydrophylicity of amide linkage leads to moisture absorption by all aramids. The skin-core structure of the *p*-aramid fibers plays an important role in the moisture absorption, which is critical for many structural applications of the FRP on their basis. Thus, Fukuda and Kawai found that the ultrahigh modulus Kevlar 149 has a moisture uptake of ~1% (20 °C, 55% relative humidity), while in the regular brand Kevlar 29 it is ~7% under the same conditions [34]. Apparently, above a certain concentration, the water molecules could upset the intermolecular hydrogen bond formation (Figure 8.2) and affect the mechanical properties, as seen by the comparison of the mechanical properties of Kevlar 29 and Kevlar 149. The same authors found that the diffusion coefficient through the skincore structure of the Kevlar fiber is also of importance; in the skin the trend is Kevlar 149 > Kevlar 29 > Kevlar 49 and in the core it is reversed: Kevlar 29 > Kevlar 49 > Kevlar 149.

p-Aramid fibers display weak compression properties, which was attributed to limited lateral cohesion between the rigid molecular chains. Between the single macromolecules there exist hydrogen bonds in one direction and van der Waals forces at right angles (Figure 8.2). Compressive stresses can therefore initiate adverse shearing or delamination of adjacent chains [35]. The lateral bonds can also affect potential water uptake that can obviously affect other physical properties.

The compression shortcomings of PPTA fibers are usually seen in the form of kink bands representing protrusions or dislocations on the fiber surface typically observed under axial compression or during tensile failure [36]. Although the reason for kinking under compression is still not well understood in general, there are indications that it is related to buckling of *p*-aramid molecules due to a molecular rotation around the amide carbon-to-nitrogen, changing the configuration from *trans* to *cis* [37]. This results in a yielding to the imposed stress without any bond cleavage. A two-dimensional model describing the initiation of kinking was recently adapted for use in PPTA fibers, whose conclusions and predictions compare favorably with the experimental results [38].

The low compressive strength was recognized as the major weak point of aramids since they were first made. The future of the *p*-aramids will be definitely related with increased research efforts to find ways to improve this weakness of PPTA without compromising on their superb tensile properties. In order to do so, both chemical modification of the polymer backbone and cross-linking between adjacent macromolecules were tried [39]. The synthesis of reactive PPTA oligomers containing reactive methacrylate and maleimide end groups and their use as lyotropic spin-dopes of conventional PPTA in a 20:80 proportion have been described recently [40]. This resulted in a modest increase (+0.1 GPa) of the compressive strength. The authors also recognized that a high-temperature treatment of the conventional PPTA fiber improves its compressive behavior much more significantly.

Other attempts to enhance lateral interactions *via* interchain interaction rely on the addition of copolymer units able of hydrogen bond formation in two directions rather than on changing the polymer backbone chemistry. The most successful attempt at present

is the development of a new polymer, PIPD-M5 (Scheme 8.1), which is capable of forming a two-dimensional hydrogen bonded network. As a result of the better lateral interactions between polymer chains, compressive strengths as high as 1.7 GPa were reported [41]. This polymer is rather expensive and the compressive properties appear to be sensitive to water, which reduces compressive performance over time [42]. The authors identify the upsetting of the intermolecular hydrogen bond formation as the reason for this effect. The original degree of H-bonding and compressive strength could be recovered by re-annealing the fiber under tension.

The PPTA-benzimidazole copolymer fibers of the SVM family (Scheme 8.1) that contain one NH group in its benzimidazole linkage in addition to the one in the amide linkage thus enabling denser intermolecular H-bond formation, has shown impressive mechanical properties. Thus, according to Slugin *et al.* [43], while the best Kevlar and Twaron brands show relative tenacities of 110–140 cN/tex and modulus values of 120–145 GPa, the Armos fibers, developed in 1978, retain higher relative tenacity (190–240 cN/tex) and high modulus (110–160 GPa) for 15 years and more and can be used in materials heavily loaded for a long time. The Rusar copolymer fibers developed in 1996 display even higher relative strength (230–300 cN/tex) and elasticity moduli of up to 140 GPa. This material is predominantly used in ballistic protection. The structural difference between Armos and Rusar apparently resides in an unspecified relation difference of PPTA/benzimidazole units. Perepelkin *et al.* [44] compared the thermal characteristics of homopolymer PPTA fibers (Twaron, Terlon and Kevlar) with those of the heterocyclic *p*-aramides (Armos, Rusar). Very small differences were found in the thermal characteristics of these two groups of *p*-aramids, the only exception being the very high LOI of the benzimidazole fibers (43–45%) against 27–29% for the Kevlar and Twaron fibers.

It is worth noting that the better performance of the Armos and Rusar fibers comes at very elevated price related with the high monomer costs, lower productivity spinning process and large energy consumption. These products apparently still do not meet the Western standards as far as quality and uniformity are concerned [45] but nevertheless could be a basis for future *p*-aramid fiber improvements.

Reinforcement of PPTA fibers with 0.5 wt% of single-wall nanotubes (SWNT) has been tried very recently by Deng *et al.* [46]. The composite fibers were spun with a dry-jet wet spinning process and characterized by Raman spectroscopy. Relative intensity of nanotube G-band and PPTA 1610 cm^{-1} peak showed a good dispersion of nanotubes in the fiber. The nanotubes improved the orientation of polymer in the composite fiber with a draw ratio of 2 but degraded the orientation for higher ratios. According to the authors, the frictional sliding in the PPTA/SWNT composite fibers resulted in improved energy dissipation and this may be useful in structural damping applications. Unfortunately, no results of mechanical testing are reported in this work.

Understanding the macroscopic physical and mechanical properties of *p*-aramid fibers as a function of temperature and strain requires an understanding of how temperature influences its microscopic structure. The recent work of Davies *et al.* [47] investigated lattice distortions in single Kevlar 29 fibers using the high brilliance of a synchrotron radiation microbeam. Lattice distortions were studied over a temperature range of 110–350 K, considering also the influence of tensile deformation. The results revealed linear thermal

expansion behavior for all unit cell axes, in general agreement with literature. Expansion/contraction is greatest along the [100] direction while being reduced along [010] by interchain hydrogen bonding. During macroscopic deformation, longitudinal crystal strain dominates with respect to axial lattice distortions induced by temperature changes. There is only a small change in the [100] coefficient of thermal expansion, with the [010] and [001] directions being largely unaffected.

8.6. Properties of *p*-aramid fiber reinforced polymer composites

It has been recognized that in high performance fiber reinforced polymer composites, *p*-aramid fibers are of major significance as reinforcing material, followed by the fibers from extended-chain flexible polymers such as Spectra® and Dyneema® [48]. The thermotropic liquid crystalline polymers (*e.g.*, Vectran®) so far seem to be of less commercial importance. Along with these polymer fibers, there also exist the carbon fibers and a number of inorganic fibers and whisker types (Table 8.1). It is worth noting that the polymeric fibers are highly oriented, while inorganic fibers are mostly isotropic. Fiber reinforcements can be used in continuous (long fibers) as well as in discontinuous (short fibers) form.

To prepare the FRP composite, the respective fiber is embedded in a polymer matrix mostly thermoset or thermoplastic resins. The role of the matrix is (i) to bind the fibers together, (ii) to transfer stresses between fibers, and (iii) to protect them against environmental attack and damage due to mechanical abrasion. The matrix also controls the processability, the maximum service temperatures, as well as the flammability and corrosion resistance of FRP. Most FRPs are made in order to improve mechanical performances such as elastic properties (modulus of elasticity) and ultimate properties (strength, toughness). To some extent and based on the choice of constituents, preparation of composites makes it also possible to tailor other physical properties, such as electrical conductivity, mass transport properties, heat conduction, *etc.* [49].

Due to space limitations, in this section only a short representation on the properties of the *p*-aramid composites comprising thermoset and thermoplastic matrices will be made, focusing mostly on the most recent scientific publications. For a most comprehensive coverage of this vast topic the corresponding references will be indicated.

8.6.1. *p-Aramid FRPs with thermoset matrices*

In general, polyester, vinyl ester and epoxy resins are the most common matrices used for the preparation of fiber-reinforced composites.

8.6.1.1. *Unsaturated polyester and vinyl ester matrices*

Unsaturated polyesters (UP) are by far the most widely used resins in the composite industry [49]. UP resins are used in the highest volume due to their relatively low cost and good combination of thermo-mechanical properties and environmental durability. Typical properties of a cast UP resin are reported in Table 8.2. A UP resin is usually obtained from unsaturated polyesters dissolved in a reactive monomer. Unsaturated polyesters are linear polymers obtained by a condensation reaction between three chemical species: saturated aromatic acids, unsaturated acids (maleic anhydride, fumaric acid), and glycols

Table 8.2. Typical properties of the three most important thermoset resins used in FRP composites (adapted from [49])

Property	Unsaturated polyester	Vinyl ester	Epoxy resin
Density (g/cm^3)	1.10–1.40	1.12–132	1.2–1.3
Tensile modulus (GPa)	2.10–3.45	3.0–3.5	2.75–4.10
Tensile strength (MPa)	34.5–103.5	73–81	55–130
Strain at break (%)	1–5	3.5–5.5	1–8
Linear thermal expansion coefficient, (10^{-6}C^{-1})	55–100	–	50–80
Heat distortion temperature, (°C)	60–205	93–135	70–170
Cure shrinkage, (%)	5–12	5.4–10.3	1–5
Water sorption in 24 h (%)	0.15–0.60	0.01–0.20	0.08–0.15

(ethylene, propylene, diethylene glycol). The resulting polymeric liquid is dissolved in a reactive diluent containing carbon-carbon double bonds, such as styrene, which reduces its viscosity, making it easier to process, and acts as molecules. The curing reaction is initiated by suitable radical initiators [49].

Vinyl ester resins are obtained by using unsaturated vinyl ester resins produced from the reaction between an unsaturated carboxylic acid (*e.g.*, methacrylic or acrylic acid) and an epoxy resin. A vinyl ester molecule contains carbon-carbon double bonds only at the ends and they are suitable to be dissolved in a reactive monomer (styrene) like UP resins. Styrene reacts with the vinyl ester resin to form cross-links at the points of the double bonds. Major advantages of vinyl ester resins with respect to UP resin is the lower susceptibility to chemical attacks and then lower cross-link density, which account for the higher strain at break. However, the volumetric shrinkage of vinyl ester resins is very high, being in the range of 5–10% (Table 8.2) [49]. For more details about unsaturated polyester and vinyl ester resins, consult the reviews of Launikitis [50], Updegraff [51] and Cassis and Talbot [52]. The earlier work of Piggot and Harris [53] compared the compression strength of carbon-, glass- and Kevlar 49 reinforced polyester resins. At a volume fraction of 30%, the Kevlar fiber composites displayed compression modulus and strength values much smaller than those in tensile mode, while carbon fiber composites were only slightly less stiff and weaker in compression than in tension. The authors showed also that the chemical composition of the matrix resin has little or no effect on the composite strength, except as a result of its effect on the matrix yield strength. Epoxy resin, however, gave a greater strength than expected, while a polyester containing ethylene glycol gave a lower strength. Such results explain why the great deal of effort is directed toward *p*-aramid thermoset composites with epoxy matrices.

8.6.1.2. *Epoxy resin matrices*

The FRPs for demanding structural applications comprising continuous *p*-aramid fiber reinforcements are most frequently based on epoxy matrices [54–56]. The main reasons

for this are mostly related to the broad range of properties achievable through a proper combination of epoxy resin and curing agent, the better adhesion to the *p*-aramid fiber reinforcements (as compared to the oriented polyethylene fibers), the low shrinkage after curing of the epoxy matrix, and its elevated resistance to chemicals and good insulating properties. Characteristic properties of a typical fully cured epoxy resins are reported in Table 8.2. It can be seen that the mechanical resistance of most epoxy resins after curing is better than of the polyesters, which was experimentally confirmed for FRPs reinforced with different polymer long fibers [53].

As already mentioned, a generic limitation of all aramid fibers is their low compressive strength. In order to avoid insufficient strength in nonaxial direction in the respective FRP composites, high levels of fiber-matrix adhesion would be required. The bonding mechanism of *p*-aramids with epoxy matrices has been reviewed in detail by Kalantar and Drzal [57] displaying the state-of-the-art until 1990. The authors concluded that off-axis properties of these composites are generally improved by significantly increasing the bonding at the fiber/epoxy matrix interface, while fracture toughness and impact resistance usually increase at low adhesion levels. The adhesion achieved between aramid fibers and epoxy matrices were much lower than that obtained by other, inorganic reinforcing fibers. In their own study on the bonding mechanism between aramid fibers and epoxy matrices, Kalantar and Drzal [58] showed that epoxy resin shrinkage is not a primary cause of sometimes insufficient adhesion of aramid fibers to epoxy matrices and that the curing temperature does not influence the composite failure mechanism. The close match of aramid radial thermal expansion coefficient and its Poisson ratio to those of the matrix reportedly results in lower interfacial radial stresses for the aramid fiber-epoxy interface, as compared to carbon fiber-epoxy interface. Furthermore, the aramid/epoxy interfacial failure involves failure by fibrillation at the fiber outer surface. This observation suggests the presence of a cohesively weak layer on the fiber exterior that can fail at low shear levels resulting in low values of interfacial shear strength and consequently in insufficient fiber-matrix load transfer. The formation of this weak layer seems to be a direct consequence of the skin/core structure of the *p*-aramid fiber.

Another valuable review on interfacial properties in aramid-epoxy composites studies the utility of the conventional micromechanics methods and Raman spectroscopy [59]. It has been demonstrated how this technique can be used to monitor the variation of fiber strain along the aramid fiber inside an epoxy resin matrix from which the interfacial shear stress can be derived. The strain-dependent shift of the 1610 cm^{-1} aramid Raman band can be used to determine the point-to-point variation of axial fiber strain along aramid fibers embedded in epoxy resin matrices from which the interfacial properties can be derived. The interfacial properties of aramid/epoxy model composites have been determined using Raman spectroscopy where the properties of the fiber, including different surface treatments, and the matrix have been changed systematically. Moreover, proofs have been presented that the assumption of constant interfacial shear stress is inappropriate for determining the interfacial shear strength (ISS) in model *p*-aramid/epoxy composites. It has also been found that the maximum ISS during a pullout test occurs well before the fiber pulls out from the resin matrix. It was noticed also that the values of interfacial shear strength calculated from a saturated fiber fragmentation test were considerably lower than the maximum value of interfacial shear stress calculated prior to fragmentation.

Moreover, the maximum values of ISS derived at different loading levels, can be used to characterize the interfacial properties of aramid/epoxy model composites. It is appropriate to mention here that ISS is proportional to the fiber tensile strength and diameter divided by the final fiber fragment length [58]. Based on the Raman response of aramid fibers, a multifunctional non-destructive test was proposed for Kevlar/epoxy laminates [60]. It was used for assessing the interface integrity and the overall stress distribution in unidirectional plies. In multidirectional composites this technique can be useful for determining the strain arising due to partial and full crack growth.

Alternatively, the deformation micromechanics of single fiber embedded model composites of PPTA fibers, embedded in an epoxy resin, have been examined using synchrotron radiation [61]. Single fibers (in air) were deformed and the *c*-spacing monitored to establish a calibration of crystal strain against applied stress. Subsequently, the variation in crystal strain along fibers, embedded in the resin matrix was mapped using synchrotron microfocus X-ray diffraction. Raman spectroscopy was then used to map molecular deformation on the same samples (recorded as shifts in the Raman band wave number) in order to provide a complementary stress data. A shear-lag analysis was conducted on the axial fiber stress data in order to calculate the ISS and identify different stress-transfer modes at fiber/resin interfaces. The results establish that the axial fiber stress distributions measured by synchrotron microfocus X-ray diffraction correlate well with those obtained using Raman spectroscopy. The interfacial shear stress data derived from the stress-transfer profiles also showed a good degree of correlation.

A significant number of studies on *p*-aramid/epoxy systems are related with surface treatments of the reinforcing fibers. The purpose of these treatments is threefold: (i) roughening of the fiber surface in order to enlarge the physical interface with the matrix resin allowing also for mechanical anchoring, (ii) chemical activation of the fiber surface, and (iii) creating chemical bonds across the fiber/matrix interface.

In their review on the application of plasma technologies for improving the properties of FRP composites, Li *et al.* [62] indicated a number of studies regarding *p*-aramid/epoxy composites. Thus, after air plasma treatment of Kevlar fibers, the ISS values of the epoxy composite increased by 45% [63]. The impact of NH_3, O_2 and H_2O plasmas on the surface properties of *p*-aramids and their adhesion with epoxy matrices were also studied considering the ISS [64,65], showing a similar improvement by 43–83% as measured by the microbond pullout technique, whereby the fiber strength was only little affected (less than 10% loss). These effects were related with the formation of various chemical functionalities upon the fiber oxygen and nitrogen containing groups.

In order to investigate the effect of oily finish materials on the interfacial strength of aramid-epoxy composites, Twaron aramid yarn has been treated in a one step finish process with combinations of adhesion improving (epoxy-amine) ingredients and processability improving oily materials [66]. Variations in the composite compression shear strength and transverse tensile strength as a function of the amount of oil showed an optimum oil content of 0.6–1.0%. This effect was explained by differences in the amount and distribution of epoxy, fixated to the yarn surface, which was found to depend on the oil content. It was concluded that the presence of a small amount of oil on commercially adhesion activated Twaron fibers required to improve their processing behavior can have a positive effect on the fiber/matrix adhesion.

The effect of γ-ray radiation grafting upon the surface properties of Armos fibers was investigated by means of several characterization techniques [67]. The interlaminar shear strength (ILSS) in Armos fibers/epoxy laminates, whose fiber reinforcements were radiation-treated, showed a 25% improvement as compared to that of similar composite with untreated reinforcements. The microhardness of the various components (the fiber, the interface and the matrix) in the composite with the treated fibers was higher than those in the untreated reference. This effect was explained with the increase of the concentration of the polar oxygen-containing functional groups of the treated Armos fiber surface as demonstrated by X-ray photoelectron spectroscopy analysis (XPS). Moreover, the surface of the irradiated Armos fibers became rougher, at the same time, comprising new chemical bonds, as revealed by atomic force microscopy (AFM) and Fourier transform infrared spectral techniques (FTIR), respectively.

Certain studies on *p*-aramid/epoxy FRP composites deal with diverse chemical surface treatment of the reinforcing fibers: bromination and metalation [68], treatment with phosphoric acid solution [69], surface modification by Friedel-Crafts type reactions [70] or with small amount of rare earths [71]. Application of organic solvents [72] and coating of the *p*-aramid with aliphatic polyamides [73] have also been investigated. The impact on the mechanical properties of the FRP composite is variable. Thus, bromination and metalation increases the ILSS values in the respective laminate composites with 812%. Surface modification by Friedel-Crafts processes results in a 50% increase of ISS, while the composite tensile strength was not negatively affected. This result was ascribed to the formation of optimum amount of stable chemical bonding between the curing reagent and active epoxy groups on the lateral chain of aramid polymer molecule. Treating the fiber with acetic anhydride followed by subsequent washing with methanol resulted in a 60% enhancement of the ILSS, however the authors [72] did not provide information about possible negative impact on the composite tensile strength. Even more effective was the treatment with 10% H_3PO_4, resulting in a growth of ILSS from 15 to 32 MPa and of the flexural resistance (measured by the critical stress intensity factor) from 12 to 23 MPa.cm$^{1/2}$. All these studies [68–73] show that the surface treatment of aramid fibers (with the exception of polyamide 6 fiber coating) is a good way of improving the adhesion at the fibers/epoxy matrix interface.

Theoretical predictions of the interfacial shear stress distribution along the interface have been made by several authors, notably Cox [74], for the case where both matrix and fiber are assumed to be linear elastic and the fiber-matrix interface remains intact. In reality, however, as the tensile loading on the specimen increases, the ISS reaches a critical value for the system. Beyond this point one or more modes of interfacial failure are observed experimentally. In Kevlar/epoxy composites, matrix yielding at the intact interface has been observed [75]. In the study of Nath *et al.* [76] elasto-plastic finite element analysis has been used to model a single unsized Kevlar 49 fiber embedded in an epoxy matrix subjected to tensile loading. The predicted axial stress distribution along the fiber is compared with experimental data, obtained using the technique of laser Raman spectroscopy, for a number of incremental applied strain levels. The geometry of the fiber end has been modeled employing an analytical fiber end fibrillation model. Furthermore, the influence of residual stresses in the system due to epoxy matrix curing has been also analyzed. Good correlation was obtained with the experimental data and it was shown

that the mode of interfacial failure in the composite involves yielding at the fiber-matrix interface initiating at their fiber end.

The absorption of water, so typical for PPTA, has been reported to affect the mechanical properties of *p*-aramid/epoxy composites. Results include up to 14% increase in tensile strength [77,78], a 15–40% decrease in flexural strength [79,80] and a 35% decrease in transverse strength [81]. Increases in tensile strength are attributed to plasticization of the resin, enabling fiber re-orientation. Decreases in flexural strength are due to a degraded fiber-matrix interface promoting delamination [79] and matrix plasticization allowing filament buckling to occur [80]. In transverse tension, moisture reduces the skin/core bonding strength of the fibers, allowing the skins to be pulled away. It also facilitates internal filament cracking through the pre-existing defect structure which exists in the fibers [81]. In addition, in fatigue, the fiber/epoxy matrix interface is degraded and more fiber splitting occurs in the moisturized samples [78]. Thus the results are generally attributed to increased plasticization of the epoxy resin and a change in fracture mechanism of the aramid fibers. NMR measurements of the quantity of water absorbed by dry Twaron PPTA yarn suggested that the water is absorbed into the voids in the fibers [82]. The results of this study seem to support a model in which the voids in the dry fibers contain a sodium salt, largely made up of sodium carbonate. During hydration, these voids become filled with water. Depending on the fraction of the pore initially filled by the salt, the absorbed water may either partially or fully dissolve the salt.

Most FRP composites contain only one type of reinforcing fiber. However, it is possible to combine several types of fibers in one matrix, producing in this way a *hybrid composite*. Through judicious combinations of different fibers, the mechanical properties of the hybrid composite can be varied over a wide range. Composite materials containing exclusively *p*-aramid fiber reinforcements, for example, are known to be far more damage resistant than carbon-fiber-reinforced plastics [83]. By combining aramid and carbon fibers, one can take advantage of the damage resistance of the aramid fibers and still retain a considerable part of the strength and stiffness of the carbon fibers, while diminishing the insufficient compressive properties of aramid composites. Where economy is important, the less expensive glass fibers may be combined with aramid fibers without seriously degrading the mechanical properties of the composite, especially when the material is to be used only under isothermal conditions and is not subjected to internal stresses due to varying thermal expansion coefficients of the fiber. Thus, for example, Stumpf *et al.* [83] simulated stress rupture in S-glass/Kevlar 149 hybrid microcomposites reviewing also the previous research in this area until 1995. White *et al.* studied such carbon fiber/Kevlar/epoxy composites using both numerical simulations and experimental characterizations during hypervelocity impact [84]. The fracture toughness behavior of carbon fiber/epoxy composite with Kevlar reinforced interleave have been studied by Yadav *et al.* [85]. The impact response of various epoxy matrices reinforced by Kevlar/carbon and glass/Kevlar fibers were studied in [86]. Apparently, besides experimental and purely analytical approaches, computer simulations will be a valuable means for the future exploring of the hybrid FRP composites necessary in order to better understand their structure-properties relationship.

Drilling and machining of *p*-aramid/epoxy composites is not straightforward, mostly because of the high toughness and flexibility of the reinforcing fibers. The study of Bhattacharyya and Horrigan [87] describes an investigation on drilling of Kevlar/epoxy FRP

composites with normal and modified drill bits under cryogenic and ambient temperatures. The delamination results have been analyzed using linear-elastic fracture mechanics and three-dimensional finite-element models. According to this study, delamination can be minimized by using a back support during drilling. The poor surface quality and edge damage at the entry and particularly at the exit faces of the drilled holes can be minimized by the application of liquid nitrogen and are totally eliminated by the introduction of very thin, resin-rich layers on the laminate surfaces. Small, blind *via* holes can be rapidly drilled in multilayer printed wiring boards, based on epoxy matrices reinforced by Kevlar or glass fibers by means of a pulsed CO_2 laser [88], leading to a significant reduction of the fabrication time.

8.6.1.3. *Other thermoset matrices for p-aramid composites*

Other thermosetting resins used as matrices for structural composites are phenolics [89], aromatic polyimides [90], and other special high-temperature, high-strength resins like bismaleimides and cyanate esters [91]. Typical properties of these resins are reported in Table 8.3.

Table 8.3. Typical properties of phenolics, polyimide, bismaleimide and cyanate ester thermoset resins (adapted from [40])

Property	Phenolics	Polyimide [a)]	Bismale-imide [b)]	Cyanate ester [c)]
Tensile modulus (GPa)	3.50	3.20	4.30	3.20
Tensile strength (MPa)	50-55	55	82	88
Strain at break (%)	1.7	1.5	2.3	3.2
Glass transition temperature (°C)	–	335	295	289

Notes: [a)] PMR 15 (Huntsman); [b)] Matrimid 5292 (Huntsman); [c)] AroCy B (Huntsman)

Generally, phenolic resin-based FRP composites yield low levels of smoke and combustion products under both flaming and smoldering fire conditions and are superior in terms of other flammability properties to polyester, vinyl ester and even epoxy-based composites. However, their mechanical properties are inferior to those of polyester, vinyl ester and epoxy due to incompatibility with reinforcing fibers finishes, typically developed for polyester or epoxy resins. Apparently, this problem can be overcome by using aramid fibers for reinforcement that have been treated in ammonia and oxygen plasma to enhance adhesion to resole phenolic resins [92]. The plasma treatments of the fibers resulted in significant improvements in ILSS (*ca.* 60%) and flexural strength (*ca.* 70%) of laminate composites made from these materials. For the composites containing oxygen and ammonia plasma-treated fibers, the enhanced ILSS and flexural strength are attributed to improved wetting of the surface-treated aramid fibers by the phenolic resin. However, for those containing fibers with reacted epoxide groups on the ammonia plasma-treated fiber surfaces, the enhanced composite properties may be due to covalent chemical interfacial bonding between the epoxide groups and the phenolic resin.

The bismaleimides (BMI) are well known as high-temperature-resistant polymers (Table 8.3). These resins are suitable for use in a wide range of composite materials since they contain unsaturated double bonds that can thermally polymerize without the evolution of volatiles that cause voids. The study of Lin *et al.* [93] examined the effect of chemical treatment on the mechanical behavior of Kevlar 49 fiber/modified bismaleimide resins. The matrix was synthesized from a four ring aromatic diamine containing ether and isopropylidene linkages. The introduction of functional groups to BMI enhancing the flexibility of the matrix improved the ISS of the Kevlar/bismaleimide composites measured by means of the microbond pullout test. On the other hand, surface modification of the aramid fiber with reactive functional groups enhanced both the interlaminar shear strength and T-peel strength of the Kevlar-fiber/BMI resin system. The ILSS was markedly improved by chlorosulfonic-acid treatment (0.2% acid for 150 s) being the optimum chlorosulfonation condition.

A modified epoxy matrix for Kevlar FRP composites was produced from epoxy/polyphenylene oxide (PPO) blends cured with multifunctional cyanate ester resin [94]. The effects of the PPO content on the cure behavior in the cyanate ester-cured epoxy were investigated with FTIR. The cure reaction in the epoxy/PPO blends was faster than that of the neat epoxy system. FTIR analysis revealed that the cyanate functional group reactions were accelerated by adding PPO and that several co-reactions had occurred. Thermal mechanical analysis showed that the thermal stability of the epoxy/PPO matrix is improved by adding PPO. In the respective composites, the ISS values between Kevlar fiber and the epoxy/PPO blends are almost the same as those between Kevlar fiber and neat epoxy. The ILSS in the respective laminates increases with the PPO content, which was attributed to an increase in the composites ductility.

All-PPTA, tri-dimensional foamed consolidated FRP composite was prepared by embedding Kevlar 49 fibers in poly(*N*,*N*-di-*sec*-butyl-*p*-phenylene terephthalamide) resin [95]. The latter, on heating in the presence of benzenesulfonic acid catalyst, was dealkylated to form the PPTA matrix. In this way, Kevlar 49/PPTA molecular composites containing fiber fractions in the range of 8–40% by volume, having densities in the range of 0.2 to 1.2 g/cm^3, were prepared and their thermal and mechanical properties characterized. It has been pointed out that such all-PPTA composites mimic natural materials, *e.g.*, the foamed composites prepared in this work had a remarkable resemblance to wood, with the advantages of flame and rot resistance.

The recent work of Kim *et al.* [96] discloses the structure and the electrical properties of PPTA/multiwalled carbon nanotubes (MWCNT) composites obtained by *in situ* polymerization. These composites exhibited improved electrical conductivity. Ground PPTA/MWCN particles were shown to behave as electrorheological (ER) material. It seems that preparing of such less usual all-aramid composites or using PPTA as matrix to be reinforced by CNT may be an interesting pathway toward composite materials, requiring, however, improved manufacturing processes.

8.6.1.4. *Manufacturing of p-aramid composites with thermoset matrices*

Closing the discussion on the thermoset aramid fiber composites, it should be noted that the manufacturing (forming) techniques in the case of the most frequently used epoxy and polyester matrices are common for all thermoset composites. The selection of a proper

manufacturing or forming technique for a polymeric fiber-reinforced composite depends strongly not only on the given matrix and fiber type, but even more on the required cost-effectiveness and the desired production rate.

The first fabrication method for fiber-reinforced thermoset polymer composites was the hand lay-up technique [89]. The procedure was partially automated in a process called *spray-up*, in which chopped fibers and resin are deposited simultaneously on the open mold by a special spray gun. Very important for the fabrication of high quality thermoset parts has become the *bag molding method*. The starting product is called *prepreg*, consisting of a thin reinforcement layer (in the form of unidirectional fibers or woven cloth) impregnated with a partially cured resin (generally epoxy) to a typical fiber volume fraction of about 50%. Composite laminae are cut from the prepreg roll and positioned on each other according to the desired laminate sequence while ensuring that the fibers are aligned in the specified direction. The uncured laminate is then positioned between various membranes and release materials. By means of an autoclave, the whole assembly is then subjected to a combination of external pressure, vacuum, and heat to consolidate and densify the various layers into a compact laminate. During this curing process part of the resin initially flows out of the prepreg, thus resulting in a typical fiber volume fraction of about 60%, which is an industrial standard for many structural applications. More details about this technique are reported by various authors [97–99].

Beginning from the mid-1970s, other methods for higher production rates like compression molding, resin transfer molding, pultrusion, and filament winding were developed. The reader is encouraged to consult the review on these techniques covering the state-of-the-art until 2002 given in [49] and also the broad topic reference book on polymer composite processing [100], chapters 5, 11, and 13.

8.6.2. *p-Aramid FRPs with thermoplastic matrices*

Thermoplastic polymers are processed by increasing the temperature until transforming them into a high-viscosity liquid. When in this state, reinforcements can be added and the material can undergo injection or extrusion processes directly adapted from thermoplastics technology. Due to processing difficulties related to the very high viscosity of polymer melts, thermoplastic matrices are predominantly used to obtain short-fiber-reinforced composites. The most common thermoplastic matrices employed for the production of short-fiber-reinforced composites are polyolefins, aromatic polyesters like poly(butylene terephthalate) and poly(ethylene terephthalate), polycarbonate, *etc.* Recently, a number of commercial short and long-fiber composites based on thermoplastic matrices have emerged, in which the mechanical properties, the temperature stability, and the solvent resistance have been greatly improved by the introduction of rigid aromatic macromolecules, thus attaining performances often equivalent to or even better than the best thermosets. Examples of such matrices are polyphenylenesulfide (PPS), poly(ether ether ketone), polysulfone, polyethersulfone, polyamideimide and thermoplastic polyimide. More information about thermoplastic matrices for composite materials is reported in the review of Migliaresi and Pegoretti [49] and in the references thereof.

It should be noted that, in general, thermosetting composites have shown superiority over the majority of the thermoplastic materials with regard to longer life and sustainability

under severe environmental attacks, such as acidic condition, exposure to high temperature and so on. Advances in science and technology pose new challenges and one of them is the need to protect the environment. In the manufacture of composites, thermosetting matrices have several ecological issues because they cannot be reused or recycled. Materials that are not fully recyclable can possess adverse environmental impacts. In recent years, there has been increasing interest in the use of thermoplastic matrices for the manufacture of fiber reinforced composites. High ultimate strain, short molding cycle, recyclability and the ability of thermoplastic matrices to be remolten and reprocessed are some of the driving factors for their increasing uses [101].

More than a decade ago, the concept of composite materials comprising a thermoplastic matrix reinforced by fibers from the same or very similar polymer had been developed [102]. The interest is mainly driven by the need to avoid physical deterioration at the interface due to poor fiber/matrix adhesion properties and to achieve improved interfacial, thermal, mechanical, economical and ecological benefits. Polyamide (PA) matrices have been frequently combined with *p*-aramid reinforcements thus expecting to produce FRP composites with little or no chemical mismatch in adhesion properties. Thus, the mechanical properties of aramid/PA6 and aramid/epoxy composites and their relationships to the fiber/matrix interfacial adhesion and interactions have been investigated [101]. With the increase in processing time, tensile modulus and strength of aramid/nylon composites have increased and decreased, respectively. It has been shown that aramid/PA6 and aramid/epoxy knitted composites display comparable strengths in the course direction, albeit the former have inferior tensile strength in the wale direction. Also, aramid/nylon composites exhibited better interfacial bonding properties than those with epoxy composites, the latter showing clear fiber/matrix debonding.

A number of *p*-aramid/PA66 composites have been prepared and investigated by the Marom group [103–105]. It seems that the improvement in the longitudinal properties of unidirectional composites of this type is inversely dependent on the thickness of the PA66 *transcrystalline layer*. Composite stiffness and strength increase as the transcrystalline layer (TCL) thickness decreases. This result was taken as a valid proof of the assumption that an effective contribution of the TCL to the mechanical properties occurs only when the *c*-axis (chain axis) of PA66 in TCL is parallel to the reinforcing fiber direction [104]. Earlier work [103], however, showed by means of AFM that in similar unidirectional Kevlar/PA66 composites, radial regularity in TCL relative to the fiber axis could be observed. X-ray diffraction investigations of the isolated layer suggested that the polymer chain is oriented predominantly perpendicular to the fiber axis. In order to clarify this controversy, a microfocus synchrotron diffraction study was performed with this system without and with application of external stress, examining also the TCL morphology by means of polarizing light microscopy [106]. Microscopy studies gave evidence that in the majority of the samples, prepared at different temperatures, the aramid fibers induced a TCL with striations perpendicular to the fiber axis. Diffraction studies showed that the growth direction of lamellae in TCL is effectively independent of location, either in the radial direction or in the direction parallel to the fiber axis. The authors supposed that the specific orientation of the PA66 lamellae as they grow outwards from the Kevlar fiber surfaces might be dependent on the pressure applied during the composite sample preparation.

Anionic graft copolymerization of ε-caprolactam onto a Kevlar-49 fiber surface was carried out in order to produce chemical bonds across the PA6 matrix/Kevlar fiber interface [107]. The effects of reaction conditions on the graft yield and on the tensile strength of the fiber were investigated in comparison with those in a PA6/Kevlar fiber composite without grafting. The grafted Kevlar fiber reinforced nylon 6 composite exhibited slightly higher storage modulus values as well as higher glass-transition temperature ascribed to the higher interfacial interaction. PA12 matrices were also explored and found useful for the manufacture of aramid fiber reinforced composite by means of a dry powder impregnation process [108]. In this work, Twaron 1056 HM fibers were preimpregnated by the deposition of fluidized PA12 powder particles consolidated by heat and pressure to form continuous prepregs. Features of the PA12 powders important for the dry powder impregnation process were discussed, outlining the materials, tools and processing parameters influencing the manufacturing process.

Polyolefin-based thermoplastic matrices have also been tried in aramid fiber reinforced composites. The study of Saikrasun *et al.* [109] discloses a composite comprising a polypropylene/EPDM matrix (18:82 wt%) (trade name Santoprene, by Advanced Elastomer Systems) reinforced by PPTA short fiber in the form of pulp. It was found that Kevlar pulp with no treatment can be used to reinforce Santoprene. However, the use of hydrolyzed pulp and a small amount of maleinized polypropylene as a reactive compatibilizer improved the modulus, tensile strength, and elongation at break of the composite as revealed by dynamic mechanical tests. These results indicated a possible reaction between the maleic groups of the compatibilizer and the free amine groups on the hydrolyzed surface of Kevlar, changing the polarity of the Kevlar surface. The authors suggested that this reaction could have resulted in increased interfacial adhesion at the fiber/matrix interface leading to a better distribution of stress along the reinforcing fiber.

Recently, the thermomechanical behavior of fluorinated and oxyfluorinated Kevlar short fiber-reinforced ethylene propylene (EP) composites has been investigated [110]. The composites were prepared by melt mixing the EP and reinforcements followed by compression molding. Samples were studied by various techniques, including FTIR, dynamic mechanical tests, thermogravimetry and X-ray diffraction. These studies showed that the thermal stability, the storage modulus, the tensile stress, as well as the crystallinity of the chemically treated Kevlar fiber-reinforced EP composites, increase in comparison to those of the untreated derivative. The explanation of these favorable changes was again related to a better adhesion between the chemically treated fiber surface and the EP matrix. Microscopy studies by scanning electron microscopy (SEM) and AFM supported this hypothesis. Similar effects were observed also when syndiotactic polystyrene was used as a matrix material with the same type of chemically treated Kevlar short fibers [111].

Kevlar fibers can be used as reinforcement for wood-flour/high-density-polyethylene matrices to improve their mechanical properties. The study of Ou *et al.* [112] demonstrates that the addition of a small amount (23%) of Kevlar short fibers can cause an improvement in the tensile, flexural and impact properties of HDPE/wood composites. As expected, additional surface modification of the Kevlar fiber with organosilanes and halides resulted in a further improvement on the composites mechanical properties. This effect was ascribed to the increased interfacial compatibility between the aramid fibers and HDPE, evidenced by SEM, XPS and FTIR methods.

The incorporation of mineral fillers into thermoplastics is widely practiced in industry to improve their mechanical and gas barrier performance. It suffices to mention the clay/polymer composites. As far as the tribological behavior is concerned, however, mineral fillers can have a different effect on the material's wear resistance as either positive or harmful. It was demonstrated that the ceramic fillers can promote decomposition of thermoplastic matrices, directly related to negative changes in the wear resistance of the respective composites, governed by the mechanical and thermal effects in the inorganic reinforcement during sliding. Since traditional organic fibers of the PPTA type have lower hardness than the ceramics, it was rational to anticipate that the organic fibers would bring about weaker mechanical and thermal effects [113]. With this idea in mind, composites of PPS reinforced with short Kevlar 29 fiber were prepared by compression molding. The friction and wear behavior of the composites was examined with a pin-on-disc test rig. It has been found that the inclusion of Kevlar fiber increases the wear resistance of PPS considerably. During the friction, a discontinuous and thick transfer film forms on the counterface against unfilled PPS while a thin and uniform transfer film is generated on the counterface against the composite with 30% Kevlar fiber. Moreover, according to the authors, Kevlar fiber as a reinforcing agent promotes the decomposition and oxidation of the polymer matrix by way of increasing the frictional heating and the wear face temperature. This helps to increase the bonding strength of the transfer film on the counterface, and subsequently increases the wear resistance of the Kevlar reinforced PPS composites [113].

Another high-performance thermoplastic material, namely poly(phthalazinone ether sulfone ketone), PPESK, was reinforced with Twaron PPTA short fibers, with and without treating the reinforcement with air dielectric barrier discharge plasma (DBD) [114]. Results show this specific plasma treatment is responsible for the introduction of reactive functional groups such as CO, O=C and O=CO. According to the authors, the DBD plasma increases the surface roughness and effectively removes the oily finish on the original fiber surface. All these effects most probably account for the noticeable enhancement of the interfacial adhesion between treated fibers and PPESK matrix and confirm the previously mentioned effect of plasma on aramid fibers used in epoxy-based FRP composites [62–65].

8.7. Concluding remarks

The discussion on the preparation and properties of *p*-aramid FRP composites should not omit the most famous application of these materials in ballistic protection. A great deal of the freely available information in this area is included in numerous patents and technical publications. Significantly less in number are the scientific articles, most frequently dealing with modeling studies. Even a brief overview on the *p*-aramid composites in ballistics would probably require a separate chapter. Due to space limitations, we will only mention here a recently reported phenomenon with big potential for more flexible and better protecting body armor in the future.

As previously mentioned, only *p*-aramid fibers (mostly Kevlar, Twaron), along with the UHMWPE (Spectra, Dyneema) have been introduced as base materials for ballistic protection. These high performance fibers are characterized by low density, high strength, and high energy absorption. However, to meet the protection requirements for typical ballistic threats, approximately 20–50 layers of fabric are required. The resulting bulk

and stiffness of the armor limits its comfort, and has restricted its application primarily to torso protection.

To eliminate this restriction, the PPTA fabrics in the layers can be impregnated with non-Newtonian fluids that exhibit the so-called shear thickening effect. At low strain rates associated with normal motion of the wearer, the shear-thickening fluid (STF) will offer little impediment to fabric flexure and deformation. However, at the high strain rates associated with a ballistic impact event, STF will thicken and in doing so, enhance the ballistic protection of the fabric. The use of this phenomenon for ballistic protection was published for the first time in 2003 [115]. This study reports on the ballistic penetration performance of a composite material composed by various layers of woven Kevlar fabrics impregnated with a STF, comprising silica particles (450 nm) dispersed in ethylene glycol. According to the authors, the addition of STF to the fabric results in a significant enhancement in ballistic penetration resistance without any loss in material flexibility. Furthermore, under the same ballistic test conditions, the impregnated fabric targets perform equivalently to neat fabric targets of equal areal density, requiring significantly less thickness – 10 instead of 31 fabric layers. The enhancement in ballistic performance is shown to be associated with the shear thickening response, and possible mechanisms of fabric-fluid interaction during ballistic impact were identified.

Summarizing, the future of aramid fibers for FRP composites seems to be related with new chemistries (homo- and copolymeric), involving stronger interactions between the macromolecules in a lateral direction, new surface treatments of the fibers for enhancing their compatibility and adhesion with the matrix, new high-performance thermosets and thermoplastics used as matrices, as well as application of the newest achievements in nanotechnology and rheology to obtain stimuli-response materials. Most probably, the application of hybrid reinforcement (*i.e.*, aramid-carbon fibers or aramid-glass fibers, *etc.*) could provide more versatile materials necessary for the future automotive, aerospace, electronic and electric industries. The future aramid composites will be a balanced result of the fundamental research on their structure-property relationship and the constant trade-off between functionality, processability and price. These have been and probably will be an ongoing challenge with these advanced materials.

Acknowledgements

N.D. is grateful to Fundação para a Ciência e Tecnologia (FCT) for post doctoral grant SFRH/BPD/45252/2008. Z.D. is grateful for the tenure of the FCT sabbatical grant SFRH/BSAB/812/2008 and for the hospitality of the Institute of Technical and Macromolecular Chemistry, Hamburg, Germany where a part of this chapter was written.

References

1. Jassal M and Ghosh S (2002) Aramid fibers - an overview, *Indian J Fiber & Text Res* **27**:290–306.
2. Chung D D L (1994) *Carbon fiber composites*, Butterworth-Heinemann, Boston, MA, p. 4.
3. Gabara V, Hartzler J D, Lee K-S and Rodini D J (2007) Aramid fibers, in *Handbook of fiber chemistry*, 3rd edition (Ed. Levin M) CRS Press, Boca Raton, FL, pp. 976–1025.
4. Bank L C (2006) *Composites for construction: Structural design with FRP materials*, John Wiley & Sons, Inc., Hoboken, New Jersey, p. 7.

5. Yang H H (1989) *Aromatic high-strength fibers*, John Wiley & Sons, New York, pp. 70–111.
6. Boerstoel H (2006) Self-organization phenomena in liquid crystal spinning, *Sen'i Gakkaishi* **62**:93–101.
7. Picken S J, Boerstoel H and Northolt M G (2006) Processing of rigid polymers to high performance fibers, in *The Concise Encyclopedia of Materials Processing* (Ed. Martin J) Elsevier Science Ltd, pp. 623–636.
8. http://www.m5fiber.com/magellan/about_magellan.htm (visited November 2010).
9. Morgan P W (1965) *Condensation polymers by interfacial and solution methods*, John Wiley & Sons, New York, NY, p. 72.
10. Gnanou Y and Fontanille M (2008) *Organic and Physical Chemistry of Polymers*, John Wiley & Sons Inc., Hoboken, New Jersey, p. 569.
11. Osawa M and Jinno M (1986) Production of totally aromatic polyamide yarn, Applicant: Mitsui Toatsu Chemicals, Japan Patent 61,201,009.
12. Higashi F, Murakami T and Taguchi Y (1982) Polyureas from carbon dioxide and amines by means of triphenyl phosphite and pyridine hydrochloride, *J Polym Sci Part A: Polym Chem* **20**:103–108.
13. Shin H (1977) Vapor-phase preparation of aromatic polyamides, Applicant: DuPont, U.S. Patent 4,009,153.
14. Singh G (1990) Melt-processible aromatic polyamides, Applicant: DuPont, EP 366316.
15. Preston J (1988) Polyamides, aromatic, in *Encyclopedia of Polymer Science and Technology*, (Eds. Mark H F, Bikales N M, Overberger C G and Menges C G) 2nd edition, Wiley Interscience, Vol. 111, New York, NY, p. 81.
16. Sweeney W (1966) Poly-meta-phenylene isophthalamides, Applicant: DuPont, U.S. Patent 3,287,324.
17. Hahn C (2000) Characteristics of *p*-aramid fibers in friction and sealing materials, *J Ind Text* **30**:146–165.
18. Blades H (1973) Dry jet wet spinning process, Applicant: DuPont, U.S. Patent 3,767,756.
19. Imanishi T and Muraoka S (1988) Transparent poly(*p*-phenylene terephthalamide) films, Applicant: Asahi Chemical, U.S. Patent 4,752,643.
20. Gross G C (1973) Synthetic paper structures of aromatic polyamides, Applicant: DuPont, U.S. Patent 3,756,908.
21. Yang H H (1993) *Kevlar Aramid Fiber*, John Wiley & Sons, Chichester, UK, p. 46.
22. Liang R, Han L, Doraiswamy D and Gupta R K (2000) Fundamental characterizations of "structured" fibrid suspensions, *Proc 13th Intern Congr Rheology*, Cambridge, UK, Aug 20–25, vol. 4, pp. 136–138.
23. Gohlke U and Baum E (1979) Fibride aus aromatischen polyamiden, *Acta Polymerica* **30**:170–175.
24. Pinzelli R and Loken H (2004) Honeycomb cores: from Nomex to Kevlar aramid papers, *JEC Composites* **8**:133–136.
25. Tsimpris C W, Wartalski J and Ferradino A G (2001) Compounding with *p*-aramid fiber elastomers, *Rubber World* **224**:35.
26. Askeland D R (1989) *The science and engineering of materials*, 2nd ed., PWS-Kent Publishing Co., Boston, Mass, p. 591.
27. Allen S R and Roche E J (1992) Tensile deformation and failure of poly(*para*-phenylene terephthalamide), *Polymer* **33**:1849–1854.
28. Penn L (1979) Physicochemical properties of Kevlar 49 fiber, *J Appl Polym Sci* **23**:59–73.
29. Konopasek L and Hearle J W S (1977) The tensile fatigue behavior of *p*-orientated aramid fibers and their fracture morphology, *J Appl Polym Sci* **21**:2791–2815.
30. Panar M, Avakian P, Blume R C, Gardner K H, Gierke T D and Yang H H (1983) Morphology of poly(*p*-phenylene terephthalamide) fibers, *J Polym Sci Part B: Polym Phys* **21**:1955–1969.

31. Northolt M G (1974) X-ray diffraction study of poly(*p*-phenylene terephthalamide) fibers, *Eur Polym J* **10**:799–804.
32. Morgan R J, Pruneda C O and Steele W J (1983) The relationship between the physical structure and the microscopic deformation and failure processes of poly(*p*-phenylene terephthalamide) fibers, *J Polym Sci Part B: Polym Phys* **21**:1757–1783.
33. Dobb M G, Johnson D J and Saville B P (1977) Supramolecular structure of a high-modulus polyaromatic fiber (Kevlar 49), *J Polym Sci Part B: Polym Phys* **15**:2201–2211.
34. Fukuda M and Kawai H (1993) Moisture sorption mechanism of aromatic polyamide fibers: diffusion of moisture in poly (*p*-phenylene terephthalamide) fibers, *Text Res J* **63**:185–193.
35. Dobb M G, Johnson D J and Saville B P (1981) Compression behavior of Kevlar fibers, *Polymer* **22**:960–965.
36. Takahashi T, Miura M and Sakurai K (1983) Deformation band studies of axially compressed poly(*p*-phenylene terephthalamide) fiber, *J Appl Polym Sci* **28**:579–586.
37. Pramanik P and Chakrovorty R (2004) The unique story of a high-tech polymer, *Resonance* **9**:39–50.
38. Edmunds R and Ahmer-Wadee M (2005) On kink banding in individual PPTA fibers, *Compos Sci Technol* **65**:1284–1298.
39. Knijnenberg A (2009) Compressive failure behavior of novel aramid fibers, *PhD thesis*, University of Delft, Chapter 1, p. 3.
40. Knijnenberg A, Bos J and Dingemans T J (2010) The synthesis and characterization of reactive poly(*p*-phenylene terephthalamide)s: A route towards compression stable aramid fibers, *Polymer* **51**:1887–1897.
41. Lammers M, Klop E A, Northolt M G and Sikkema D J (1998) Mechanical properties and structural transitions in the new rigid-rod polymer fiber PIPD (M5) during the manufacturing process, *Polymer* **39**:5999–6005.
42. Leal A A, Deitzel J M, McKnight S H and Gillespie J W Jr (2009) Effect of hydrogen bonding and moisture cycling on the compressive performance of poly(pyrido bisimidazole) (M5) fiber, *Polymer* **50**:2900–2905.
43. Slugin I V, Sklyarova G B, Kashirin A I and Tkacheva I V (2006) Rusar *p*-aramid fibers for composites materials with construction application, *Fiber Chemistry* **38**:25–26.
44. Perepelkin K E, Andreeva I V, Pakshver E A and Morgoeva I Yu (2003) Thermal characteristics of *p*-aramid fibers, *Fiber Chemistry* **35**:265–269.
45. National materials advisory board, Division on engineering and physical sciences, High-performance structural fibers for advanced polymer matrix composites, The National Academy Press, Washington DC, 2005, p. 13.
46. Deng L, Young R J, van der Zwaag S and Picken S (2010) Characterization of the adhesion of single-walled carbon nanotubes in poly(*p*-phenylene terephthalamide) composite fibers, *Polymer* **51**:2033–2039.
47. Davies R J and Burghammer M (2009) Thermal- and stress-induced lattice distortions in a single Kevlar 49 fiber studied by microfocus X-ray diffraction, *J Mater Sci* **44**:4806–4813.
48. Kumar S and Wang Y (1997) Fibers, fabric, and fillers, in *Composites Engineering Handbook* (Ed. Mallick P K) Marcel Dekker Inc., New York, NY, pp. 51–100.
49. Migliaresi C and Pegoretti A (2002) Fundamentals of polymeric composite materials, in *Integrated Biomaterials Science* (Ed. Barbucci R) Kluwer Academic/Plenum Publishers, New York, NY, pp. 69–117.
50. Launikitis M B (1982) Vinyl ester resins, in *Handbook of Composites* (Ed. Lubin G) Van Nostrand Reinhold Company Inc., New York, NY, pp. 38–49.
51. Updegraff I H (1982) Unsaturated polyester resins, in *Handbook of Composites* (Ed. Lubin G) Van Nostrand Reinhold Company Inc., New York, NY, pp. 17–37.

52. Cassis F A and Talbot R C (1998) Polyester and vinyl ester resins, in *Handbook of Composites,* 2nd edition (Ed. Peters S T) Chapman & Hall, London, UK, pp. 34–47.
53. Piggot M R and Harris B (1980) Compression strength of carbon, glass and Kevlar 49 fiber reinforced polyester resins, *J Mater Sci* **15**:2523–2538.
54. Penn L S and Chiao T T (1982) Epoxy resins, in *Handbook of Composites* (Ed. Lubin G) Van Nostrand Reinhold Company Inc., New York, NY, pp. 57–88.
55. Juska T D and Puckett P M (1997) Matrix resins and fiber/matrix adhesion, in *Composites Engineering Handbook* (Ed. Mallick P K) Marcel Dekker Inc., New York, NY, pp. 101–165.
56. Penn L S and Wang H (1998) Epoxy resins, in *Handbook of Composites,* 2nd edition (Ed. Peters S T) Chapman & Hall, London, UK, pp. 48–74.
57. Kalantar J and Drzal L T (1990) Bonding mechanism of aramid fibers to epoxy matrices – a review of the literature, *J Mater Sci* **25**:4186–4193.
58. Kalantar J and Drzal L T (1990) Bonding mechanism of aramid fibers to epoxy matrices – experimental investigation, *J Mater Sci* **25**:4194–4202.
59. Andrews M C, Bannister D J and Young R J (1996) The interfacial properties of aramid/epoxy model composites, *J Mater Sci* **31**:3893–3913.
60. Parthenios J, Katerelos D G, Psarras G C and Galiotis C (2002) Aramid fibers; a multifunctional sensor for monitoring stress/strain fields and damage development in composite materials, *Eng Fract Mechan* **69**:1067–1087.
61. Shyng Y T, Bennett J A, Young R J, Davies R J and Eichhorn S J (2006) Analysis of interfacial micromechanics of model composites using synchrotron microfocus X-ray diffraction, *J Mater Sci* **41**:6813–6821.
62. Li R, Ye L and Mai I W (1997) Application of plasma technologies in fiber-reinforced polymer composites: a review of recent developments, *Composites Part A* **28**:73–86.
63. Biro D A, Pleizier G and Deslandes Y (1993) Application of the microbond technique. IV. Improved fiber-matrix adhesion by RF plasma treatment of organic fibers, *J Appl Polym Sci* **47**:883–894.
64. Sheu G S and Shyu S S (1994) Surface properties and interfacial adhesion studies of aramid fibers modified by gas plasmas, *Compos Sci Technol* **52**:489–497.
65. Sheu G S and Shvu S S (1994) Surface modification of Kevlar 149 fibers by gas plasma treatment. Part II: Improved interfacial adhesion to epoxy resin, *J Adhes Sci Technol* **8**:1027–1042.
66. de Lange P J, Akker P G, Maeder E, Gao S L, Prasithphol W and Young R J (2007) Controlled interfacial adhesion of Twaron aramid fibers in composites by the finish formulation, *Compos Sci Technol* **67**:2027–2035.
67. Zhang Y H, Huang Y D, Liu L and Cai K L (2008) Effects of γ-ray radiation grafting on aramid fibers and its composites, *Appl Surface Sci* **254**:3153–3161.
68. Lin J S (2002) Effect of surface modification by bromination and metalation on Kevlar fiber/epoxy adhesion, *Eur Polym J* **38**:79–86.
69. Park S J, Seo M K, Ma T J and Lee D R (2002) Effect of chemical treatment of Kevlar fibers on mechanical interfacial properties of composites, *J Colloid Interface Sci* **252**:249–255.
70. Liu T M, Zheng Y S and Hu J (2010) Surface modification of aramid fibers with novel chemical approach, *Polym Bull* (Published on-line 08.01, DOI 10.1007/s00289–010–0313–y).
71. Wu J and Cheng X (2005) Study of interlaminar shear strength of rare earths treated aramid fiber reinforced epoxy composites, *J Mater Sci* **40**:1043–1045.
72. Yue C Y and Padmanabhan K (1999) Interfacial studies on surface modified Kevlar fiber/epoxy matrix composite, *Compos Part B* **30**:205–217.
73. Varelidis P C, Papakostopoulos D G, Pandazis C I and Papaspyrides C D (2000) Polyamide coated Kevlar fabric in epoxy resin: mechanical properties and moisture absorption studies, *Compos Part A* **31**:549–558.
74. Cox H L (1952) The elasticity and strength of paper and other fibrous materials, *Br J Appl Phys* **3**:72–78.

75. Guild F J, Vlattas C and Galiotis C (1994) Modeling of stress transfer in fiber composites, *Compos Sci Technol* **50**:319–332.
76. Nath R B, Fenner D N and Galiotis V (1996) Elastoplastic finite element modeling of interfacial failure in model Kevlar 49 fiber-epoxy composites, *Compos Part A* **27**:821–832.
77. Komai K, Minoshima K and Shiroshita S (1991) Hygrothermal degradation and fracture process of advanced fiber-reinforced plastics, *Mater Sci Eng A* **143**:155–166.
78. Roylance M (1982) The effect of moisture on the fatigue resistance of an aramid/epoxy composite, *Polym Eng Sci* **22**:988–993.
79. Allred R E (1981) The effect of temperature and moisture content on the flexural response of Kevlar/epoxy laminates: Part II. [±45,0/90] filament orientation, *J Compos Mater* **15**:117–132.
80. Allred R E (1981) The effect of temperature and moisture content on the flexural response of Kevlar/epoxy laminates: Part I. [0/90] filament orientation, *J Compos Mater* **15**:101–116.
81. Allred R E and Roylance D K (1983) Transverse moisture sensitivity of aramid/epoxy composites, *J Mater Sci* **18**:652–656.
82. Connor C and Chadwick M M (1996) Characterization of absorbed water in aramid fiber by nuclear magnetic resonance, *J Mater Sci* **31**:3871–3877.
83. Stumpf H, Schwartz P, Lienkamp M and Schulte K (1995) S-glass fiber/Kevlar 149 hybrid microcomposites in stress rupture: a Monte-Carlo simulation, *Compos Sci Technol* **54**:211–221.
84. White D M, Taylor E A and Clegg R A (2003) Simulation and experimental characterization of direct hypervelocity impact on a spacecraft hybrid carbon fiber/Kevlar composite structure, *Intern J Impact Eng* **29**:779–790.
85. Yadav S N, Kumar V and Verma S K (2006) Fracture toughness behavior of carbon fiber epoxy composite with Kevlar reinforced interleave, *Mater Sci Eng, B* **132**:108–112.
86. Imielínska K, Castaings M, Wojtyra R, Haras J, Le Clezio E and Hosten B (2004) Air-coupled ultrasonic C-scan technique in impact response testing of carbon fibre and hybrid: glass, carbon and Kevlar/epoxy composites, *J Mater Process Technol* **157–158**:513–522.
87. Bhattacharyya D and Horrigan D P W (1998) A study of hole drilling in Kevlar composites, *Compos Sci Technol* **58**:267–283.
88. Hirogaki T, Aoyama E, Inoue H, Ogawa K, Maeda S and Katayama T (2001) Laser drilling of blind via holes in aramid and glass/epoxy composites for multilayer printed wiring boards, *Compos Part A* **32**:963–968.
89. Agarwal B G and Broutman L J (1990) *Analysis and performance of fiber composites,* 2nd edition, John Wiley & Sons, New York, NY.
90. Gibbs H H (1998) High temperature resins, in *Handbook of Composites,* 2nd edition (Ed. Peters S T) Chapman & Hall, London, pp. 75–98.
91. Shimp D A (1998) Speciality matrix resins, in *Handbook of Composites,* 2nd edition (Ed. Peters S T) Chapman & Hall, London, pp. 99–114.
92. Brown J R and Mathys Z (1997) Plasma surface modification of advanced organic fibers, Part V Effects on the mechanical properties of aramid/phenolic composites, *J Mater Sci* **32**:2599–2604.
93. Lin T K, Wu S J, Lai J G and Shyu S S (2000) The effect of chemical treatment on reinforcement/matrix interaction in Kevlar-fiber/bismaleimide composites, *Compos Sci Technol* **60**:1873–1878.
94. Wu S J, Lin T K, Zhang J X and Shyu S S (2000) Properties of cyanate ester-cured epoxy/polyphenylene oxide blends as a matrix material for Kevlar fiber composites, *J Adhes Sci Technol* **14**:1423–1438.
95. Memeger W Jr (1999) "Mimetic" molecular composites of Kevlar aramid/poly(*p*-phenyleneterephthalamide**,** *J Mater Sci* **34**:801–809.
96. Kim H S, Myung S J, Jung R and Jin H J (2008) Preparation and characterization of poly(*p*-phenylene terephthalamide)/multiwalled carbon nanotube composites via *in situ* polymerization, *Mol Cryst Liq Cryst* **492**:384–391.

97. Bader M G and Lekakou C (1997) Processing for laminate structures, in *Composites Engineering Handbook* (Ed. Mallick P K) Marcel Dekker Inc., New York, NY, pp. 371–479.
98. Sidwell D R (1998) Hand lay-up and bag molding, in *Handbook of Composites,* 2nd edition (Ed. Peters S T) Chapman & Hall, London, UK, pp. 352–377.
99. Dillon G, Mallon P and Monaghan M (1997) The autoclave processing of composites, in *Advanced Composite Manufacturing* (Ed. Gutowski T G) John Wiley & Sons, New York, NY, pp. 207–258.
100. Davé R S and Loos A C (2000) *Processing of Composites*, Hanser Publishers, Munich, Germany.
101. Khondker O A, Fukui T, Inoda M, Nakai A and Hamada H (2004) Fabrication and mechanical properties of aramid/nylon plain knitted composites, *Compos Part A* **35**:1195–1205.
102. Inoda M, Fukui T, Iwamoto M and Hamada H (1999) Mechanical properties of interface-less composites, *Polym Preprints Japan* **48**:1068–1076.
103. Klein N, Marom G and Wachtel E (1996) Microstructure of nylon 66 transcrystalline layers in carbon and aramid fiber reinforced composites, *Polymer* **37**:5493–5498.
104. Nuriel H, Klein N and Marom G (1999) The effect of the transcrystalline layer on the mechanical properties of composite materials in the fiber direction, *Compos Sci Technol* **59**:1685–1690.
105. Nuriel H, Kozlovich N, Feldman Y and Marom G (2000) The dielectric properties of nylon 6,6/ aramid fiber microcomposites in the presence of transcrystallinity, *Compos Part A* **31**:69–78.
106. Feldman A Y, Wachtel E, Zafeiropoulos N E, Schneider K, Stamm M, Davies R J, Weinberg A and Marom G (2006) In situ synchrotron microbeam analysis of the stiffness of transcrystallinity in aramid fiber reinforced nylon 66 composites, *Compos Sci Technol* **66**:2009–2015.
107. Kim E Y, An S K and Kim H D (1997) Graft copolymerization of ε-caprolactam onto Kevlar-49 fiber surface and properties of grafted Kevlar fiber reinforced composite, *J Appl Polym Sci* **65**:99–107.
108. Rath M, Kreuzberger S and Hinrichsen G (1998) Manufacture of aramid fiber reinforced nylon-12 by dry powder impregnation process, *Compos Part A* **29**:933–938.
109. Saikrasun S, Amornsakchai T, Sirisinha C, Meesiri W and Bualek-Limcharoen S (1999) Kevlar reinforcement of polyolefin-based thermoplastic elastomer, *Polymer* **40**:6437–6442.
110. Mukherjee M, Das C K and Kharitonov A P (2006) Fluorinated and oxyfluorinated short Kevlar fiber-reinforced ethylene-propylene polymer, *Polym Compos* **27**:205–212.
111. Mukherjee M, Das C K, Kharitonov A P, Banik K, Mennig G and Chung T N (2006) Properties of syndiotactic polystyrene composites with surface modified short Kevlar fiber, *Mater Sci Eng, A* **441**:206–214.
112. Ou R, Zhao H, Sui S, Song Y and Wang Q (2010) Reinforcing effects of Kevlar fiber on the mechanical properties of wood-flour/high-density-polyethylene composites, *Compos Part A* **41**:1272–1278.
113. Yu L G and Yang S R (2002) Investigation of the transfer film characteristics and tribochemical changes of Kevlar fiber reinforced PPS composites in sliding against a tool steel counter face, *Thin Solid Films* **413**:98–103.
114. Jia C, Chen P, Li B, Wang Q, Lu C and Yu Q (2010) Effects of Twaron fiber surface treatment by air dielectric barrier discharge plasma on the interfacial adhesion in fiber reinforced composites, *Surf Coat Technol* **204**:3668–3675.
116. Lee S Y, Wetzel E D and Wagner N J (2003) The ballistic impact characteristics of Kevlar woven fabrics impregnated with a colloidal shear thickening fluid, *J Mater Sci* **38**:2825–2833.